

An Upgrade for the HPS Silicon Vertex Tracker

M. Diamond, N. Graf, M. Graham, J. Jaros, T.
Maruyama, J. McCormick, O. Moreno, T. Nelson*, M. Solt
SLAC National Accelerator Laboratory, Menlo Park, CA 94025

V. Fadeyev, R. Johnson, M. Testa
University of California, Santa Cruz, CA 95064

B. Yale
University of New Hampshire, Department of Physics, Durham, NH 03824

(Dated: June 11, 2017)

*Contact person

EXECUTIVE SUMMARY

The reach of the HPS Experiment, a fixed target search for a hidden-sector vector boson, can be extended significantly with the addition of a new layer positioned between the target and the current first layer of the Silicon Vertex Tracker (SVT). Employing a small number of new techniques to build on the success of the SVT, it appears there are solutions to all of the potential issues presented by such an upgrade. Furthermore, the mechanical, cooling, power and DAQ resources required to support the additional tracking layer are already present in the current SVT. As a result, the scope of the project is small and can be undertaken with minimal resources on a short timescale. While the detector is partially disassembled to perform this upgrade, it will be possible to make small position changes to layers 2 and 3 of the SVT, to improve acceptance for long-lived A' decays.

Contents

1. Introduction and Motivation	4
1.1. The HPS Experiment	4
1.2. Improving Reach with an Additional SVT Layer	5
1.3. Acceptance Errors in Reach Estimates from the HPS Proposal	7
1.4. Improving SVT Acceptance for Long-lived A' decays	7
1.5. Physics Impact of Trigger and SVT Upgrades	9
2. HPS SVT Layer 0 Design	10
2.1. Mechanics	15
2.2. Sensors	19
2.3. Data Acquisition	19
2.4. Installation and Integration	20
3. HPS SVT Upgrade Project Outline and Scope of Work	21
3.1. Schedule	22
3.2. Budget	22
References	24

1 Introduction and Motivation

The heavy photon (A'), aka a “hidden sector” or “dark” photon, is a massive gauge boson which couples weakly to electric charge by mixing with the Standard Model photon [1, 2]. Consequently, it can be radiated by electrons and subsequently decay into e^+e^- pairs, albeit at rates far below those of QED trident processes. Heavy photons have been suggested by numerous beyond Standard Model theories [3] to explain the discrepancy between theory and experiment of the muon’s $g-2$ [4], and as a possible explanation of recent astrophysical anomalies, e.g. [5–7]. Heavy photons couple directly to hidden sector particles with “dark” or “hidden sector” charge; these particles could constitute all or some of the dark matter, e.g. [8, 9]. Current phenomenology highlights the 20–1000 MeV/ c^2 mass range, and suggests that the coupling to electric charge, ϵe , has ϵ in the range of $10^{-4} - 10^{-2}$. This range of parameters makes A' searches viable in medium energy fixed target electroproduction [10], but requires large data sets and good mass resolution to identify a small mass peak above the copious QED background. At small couplings, the A' becomes long-lived, so detection of a displaced decay vertex can reject the prompt QED background and boost experimental sensitivity.

1.1 The HPS Experiment

The HPS experiment [11] was installed in Hall-B at JLab in late 2014 and early 2015 to search for heavy photons by directing the 1.1-6.6 GeV CEBAF12 electron beam onto a thin (0.125% $X_0 - 0.25\% X_0$) tungsten target foil. The HPS experiment uses both invariant mass and secondary vertex signatures to search for A' decays into e^+e^- pairs. At CEBAF energies, the A' decay products are boosted along the beam axis with small opening angles. For couplings $\epsilon \lesssim 10^{-3}$, A' decay lengths range from millimeters to tens of centimeters and beyond. Accordingly the tracking detectors cover opening angles down to 15 mrad and are placed just 10 cm downstream of the target.

HPS employs a 90 cm long silicon tracking and vertexing detector (SVT) located inside a dipole magnet to measure momenta and decay vertex positions. A fast PbWO_4 electromagnetic calorimeter downstream of the magnet provides the trigger and electron identification.

Both the silicon tracker and the ECal have \sim ns timing resolution, which eliminates much of the out-of-time background from multiple scattered beam electrons. Fast front end electronics and high trigger and data rate capability and the near 100% duty cycle of the CEBAF accelerator allows HPS to accumulate the very large statistics needed to be sensitive to the highly suppressed production of heavy photons.

The HPS experiment completed a successful Engineering Run in Spring 2015, including a short period of production running resulting in a small physics-quality dataset at $E_{\text{beam}} = 1.06$ GeV. Subsequent analysis has shown that the performance of the detector meets the goals set in the proposal for the critical measurables of e^+e^- mass and vertex resolution that determine the experimental reach of HPS for hidden sector photons. In Spring 2016, HPS completed an engineering run at 2.3 GeV, collecting approximately 5 days of data. HPS is planning for a longer physics run in 2018.

1.2 Improving Reach with an Additional SVT Layer

The originally anticipated reach of the HPS experiment after one month of running is shown in Figure 1 [11], together with the projected reaches of other proposed experiments. Aside from the difficulty in probing masses above $\approx 2m_\mu$ the most difficult region to access is at intermediate couplings, in the range of $10^{-8} < \epsilon^2 < 10^{-6}$. While there are a number of proposals that aim to probe this region, only LHCb claims the ability to cover it completely, and not until ≈ 2023 after the completion of a major detector upgrade and collection of data during Run 3 of the LHC. While the HPS experiment is designed to take data for a total of 6 months, even with a complete dataset collected at all energies, HPS has anticipated leaving roughly one order of magnitude in coupling unexplored in the range $\approx 15\text{MeV}-150\text{MeV}$.

The reason for the gap in sensitivity at intermediate couplings is simple. For a pure resonance search, the irreducible backgrounds from radiative tridents are quite large, so only for couplings where the signal is also relatively large is there sensitivity. This situation only changes at couplings low enough that the entire prompt background can be eliminated by requiring a separated vertex. Below that, there is no background, opening up a new region of sensitivity at low couplings that extends downward in coupling until the production cross section becomes so low that there are no signal events remaining. Since collection of much

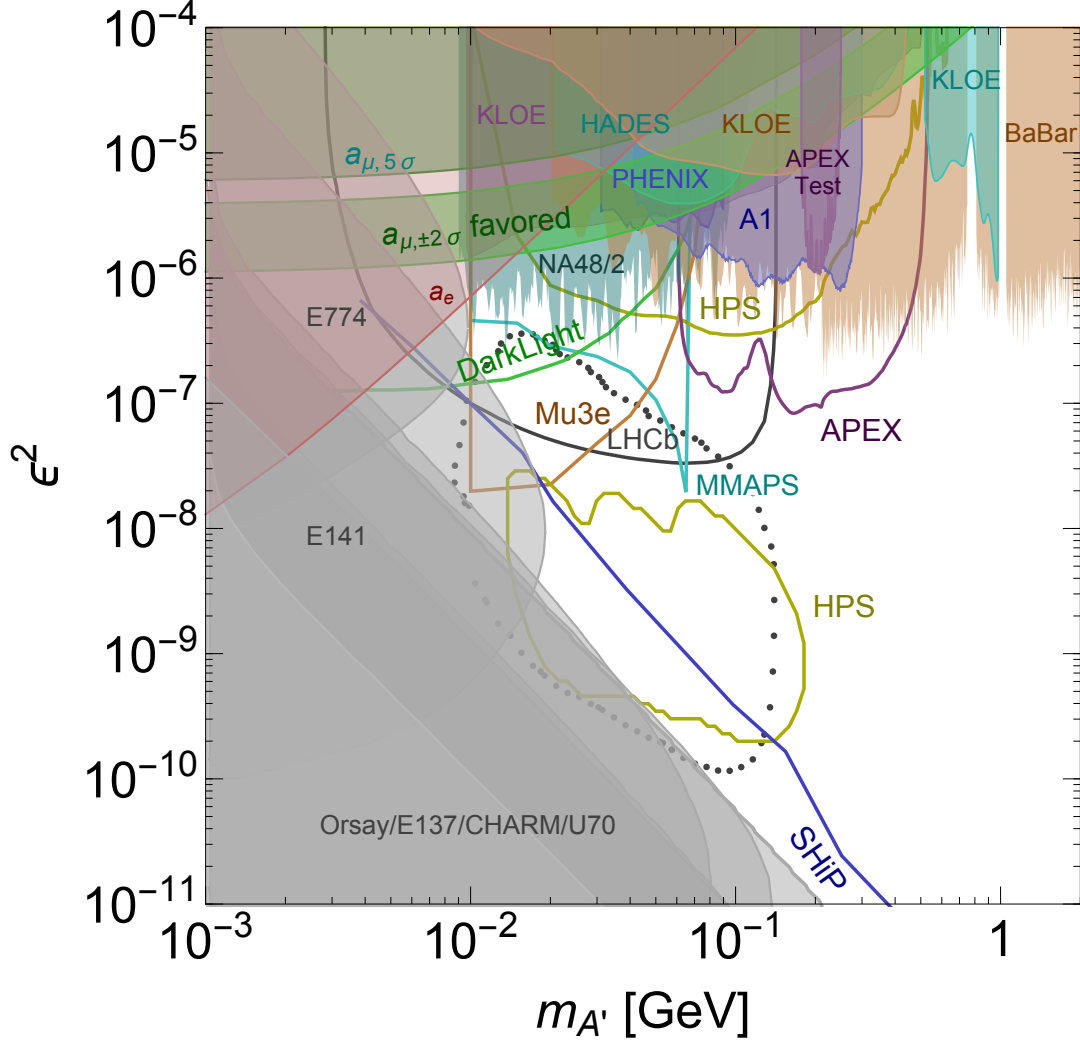


FIG. 1: The originally anticipated reach of the HPS Experiment, as per the HPS Proposal [11], for 1 month of running together with current exclusions (solid) and projected reach of other proposed experiments in the next decade.

higher statistics with HPS is impossible, the most promising avenue to close the gap at intermediate couplings is to improve the vertex resolution, which enables the elimination of prompt backgrounds at couplings larger than the proposed vertex reach. Significant improvements in vertex resolution can be achieved by adding a new SVT layer closer to the target, a project that appears possible within the framework of the current SVT, which already has facilities in place that would serve to support an additional layer, both mechanically and electrically. Therefore, we have been planning to add a new layer, Layer 0, located at $z = 5$ cm, directly between the target at $z = 0$ cm and Layer 1 at $z = 10$ cm. This additional layer would utilize thinned sensors to reduce the material by a factor of two

in comparison to the other layers of the SVT. Because the impact parameter resolution is dominated by multiple scattering in the first plane, a new layer half the distance from the target and with half the material improves the vertex resolution by approximately a factor of $2\sqrt{2}$.

1.3 Acceptance Errors in Reach Estimates from the HPS Proposal

Recently, based on preliminary analysis of the data from the 2015 Engineering Run, it has become clear that the acceptance of the detector (both ECal trigger and SVT) was not estimated correctly for the proposal, seriously overestimating the reach of the experiment, especially in the vertexing analysis. A new estimate of the reach of the installed detector has been developed based on current best understanding, conservatively assuming no further improvements to the analysis but also that no new backgrounds are uncovered at higher statistics. This reach is shown in Figure 2, where it should be noted that this estimate is for three months of total running time, triple what was assumed in the proposal but still only half of the 180 days for which HPS is approved. Without further improvements, the experiment has no reach in the vertexing analysis with these datasets. In light of this realization, the addition of Layer 0 takes on much greater importance. The dramatic increase in yields at shorter lifetimes provides much higher event yields over a large range of couplings where the A' is relatively short-lived. Meanwhile, a clear understanding of the acceptance with data motivates further changes to the apparatus to achieve acceptance closer to that assumed in the proposal. These changes include small adjustments to the SVT geometry, described in the next section, and a scintillator hodoscope for the trigger, described very briefly in section 1.5 along with updated reach projections.

1.4 Improving SVT Acceptance for Long-lived A' decays

In the reach calculations for the proposal, the acceptance for A' decays was assumed to be uniform for all A' decays occurring between the target and the first silicon layer downstream, and equal to the acceptance for prompt decays. Because the acceptance of all layers of the SVT are 15 mrad with respect to the target, downstream decays only have acceptance that begins at much larger angles. This error significantly reduces the acceptance of the

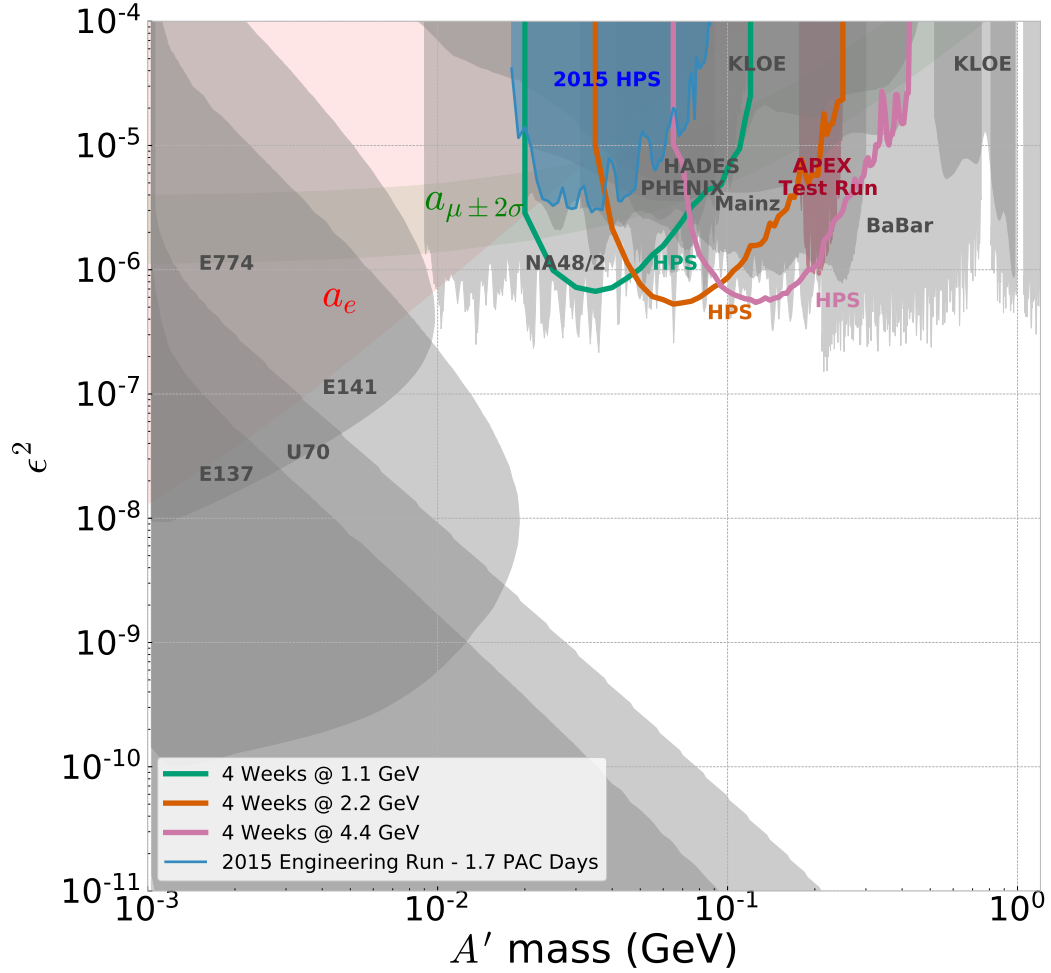


FIG. 2: The projected reach of the HPS experiment for a three month run plan consisting of four weeks each at beam energies of 1.1 GeV, 2.2 GeV, and 4.4 GeV assuming no upgrades to the detector. There is no vertexing reach in this scenario.

experiment for long-lived decays relative to the proposal, negatively impacting the reach.

When running in the nominal configuration, with acceptance in all layers beginning at 15 mrad with respect to the target, only the occupancy in the first layer limits the ability to place the sensors closer to the beam. In the deeper layers of the detector, the occupancies are lower, so that the sensors could be placed somewhat closer to the beam. In particular, if all of the other layers were moved in by 1.5 mm, the acceptance for decays at Layer 1 would indeed be the same as the acceptance for decays at the target. While backgrounds at Layer

2 only allow it to be moved by approximately 0.8 mm, moving Layers 2-6 by this amount recovers significant acceptance for long-lived A' decays.

Because Layers 2 and 3 are mounted to the same "U-channel" support structure that will hold Layer 0 and must be removed and disassembled for installation of Layer 0, it is very simple to add thin metal shims underneath the Layer 2 and Layer 3 modules during re-assembly to accomplish this move. Meanwhile, the long lever arm to Layer 4 (50 cm downstream of the target) is so long that removing and reworking the Layer 4-6 U-channel is not worth the negligible gain over only moving Layers 2 and 3. This project is small and almost entirely decoupled from the work for Layer 0.

1.5 Physics Impact of Trigger and SVT Upgrades

In addition to the error in modeling the SVT acceptance for long-lived A' daughters, the proposal also neglected to account for the removal of several crystals on the electron side of the ECal due to extreme occupancies from scattered beam electrons. Many electrons from low-mass A' are lost in this "hole", significantly degrading the vertex reach. A proposed trigger hodoscope in front of the ECal on the positron side will allow a positron-only trigger for those events, recovering much of that lost acceptance. The reach for the detector, including this positron-only trigger, but no upgrades to the SVT, is shown in Figure 3 for three months each at beam energies of 1.1 GeV, 2.2 GeV, and 4.4 GeV. The reach for the detector including both the positron-only trigger hodoscope and the proposed upgrades for the SVT for the same three month run plan is shown in Figure 4. The SVT upgrades are similar in impact to the addition of the positron-only trigger, where the vast majority of the improvement from the SVT upgrade is due to the addition of Layer 0. Clearly, these upgrades are not simply improvements to the experiment, but rather absolutely critical to the viability of the vertex reach of HPS, the heart of the experimental motivation. Because these upgrades can be undertaken at minimal cost in a very short time period, these modifications can be made quickly enough that the vast majority of the data taken by HPS will have them in place.

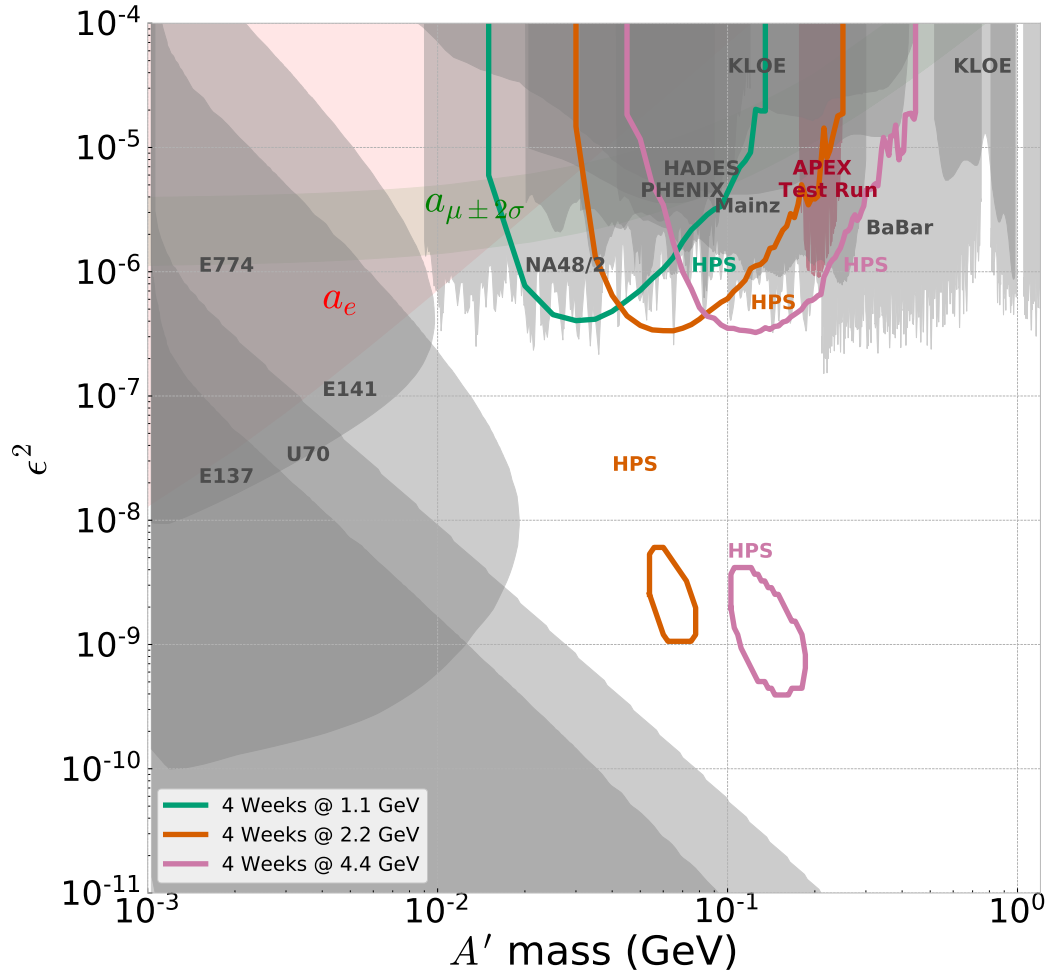


FIG. 3: The projected reach of the HPS experiment for a three month run plan consisting of four weeks each at beam energies of 1.1 GeV, 2.2 GeV, and 4.4 GeV assuming an upgrade of the trigger to include a positron trigger hodoscope (see text) but no upgrades to the SVT.

2 HPS SVT Layer 0 Design

The addition of a Layer 0 to the HPS SVT must overcome a few key obstacles. First, a layer half the distance from the target must instrument a region closer to the beamline than Layer 1 by the same factor in order to maintain the full acceptance of the SVT. Second, the use of thin silicon to reduce the material in the first layer by a factor of two reduces the signal yield in the silicon by the same factor. Finally, space and facilities inside the vacuum

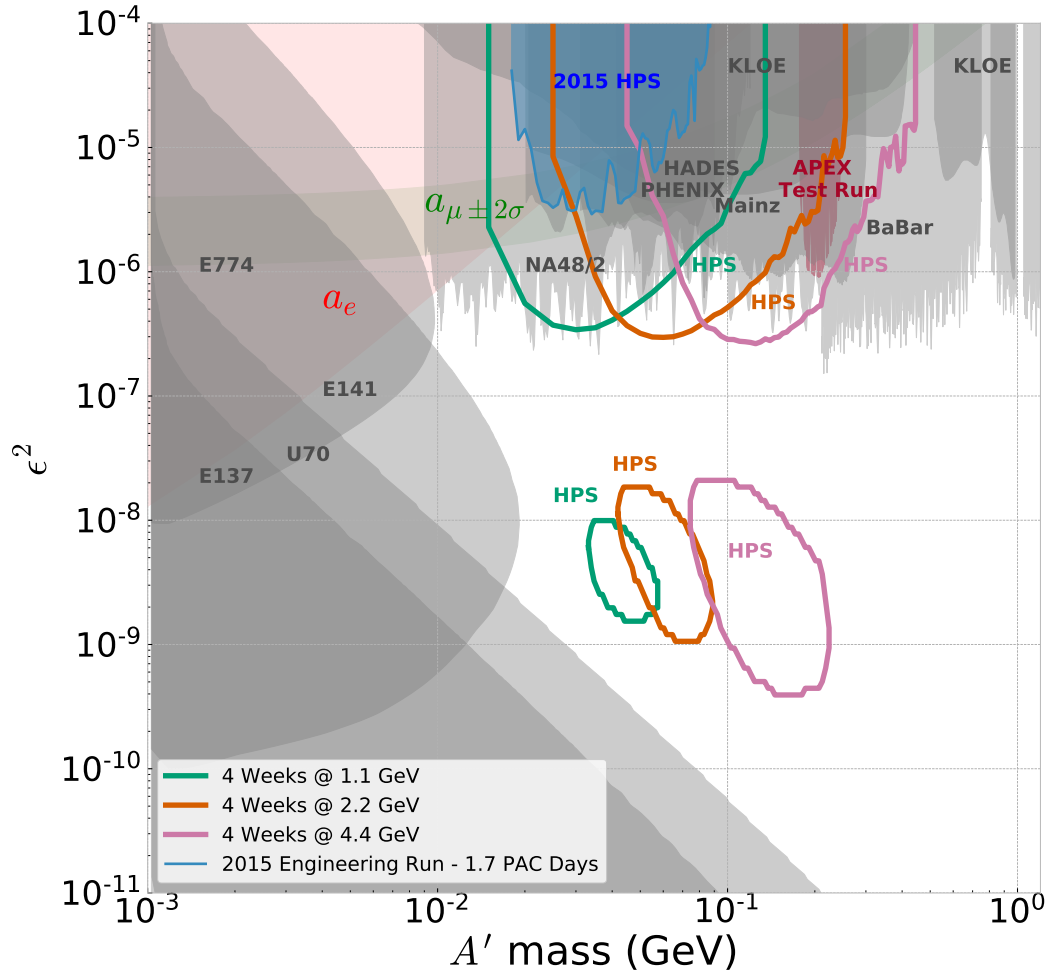


FIG. 4: The projected reach of the HPS experiment for a three month run plan consisting of four weeks each at beam energies of 1.1 GeV, 2.2 GeV, and 4.4 GeV assuming both an upgrade of the trigger to include a positron trigger hodoscope (see text) and the proposed upgrades of the SVT.

chamber limit the feasible options for addition of another tracking plane. The proposed design for Layer 0 is shaped by these requirements.

The first layer of the current SVT, Layer 1, is located at $z=10$ cm downstream of the thin tungsten target and enables angular acceptance down to 15 mrad from the beamline, necessary for sensitivity to low-mass A' decays, by placing the edge of the active silicon 1.5 mm from the beam. Utilizing standard radiation-tolerant microstrip sensors which have a ≈ 1 mm inactive border, the physical edge of the silicon in Layer 1 is therefore a mere

500 μm from the center of the scattered primary beam. Such sensors are obviously unusable for Layer 0, which must have an active region that begins 750 μm from the beamline in order to maintain the same angular acceptance when placed at $z=5$ cm. While there are a number of options for producing slim-edge sensors, the scribe-cleave-passivation processing of standard sensors can easily be used for the small number of sensors required here and has been shown to result in sensors capable of withstanding the high bias voltages needed for radiation tolerance [12].

The dominant backgrounds from scattered primary beam will be higher in Layer 0 than in the current SVT. While one might naively expect background occupancy to increase by a factor of 4 ($\propto 1/r^2$), it is important to remember that microstrips do not sample the areal density of hits. Simulation shows that background occupancy at $z=5$ cm increases by roughly a factor of 2 relative to Layer 1, as shown in Figure 5. To bring occupancies

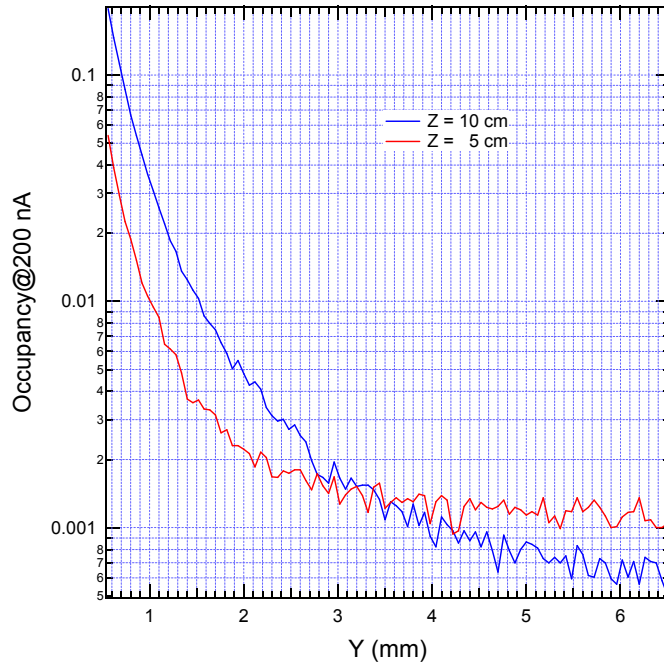


FIG. 5: The occupancy in a horizontal 60 μm readout strip as a function of vertical distance from the beam plane for sensors placed at $z=5$ cm and $z=10$ cm from the beam. The occupancy at 15 mrad for a Layer 0 at $z=5$ cm, 750 μm from the beam, is roughly $2\times$ the occupancy for the current Layer 1 with the same 15 mrad coverage, 1.5 mm from the beam.

back to acceptable levels, we propose to split the readout strips on the sensors in half so that the sensors are read out from both ends. This arrangement will cut the occupancy in

half so that they are similar to the current occupancies in Layer 1, preserving clean pattern recognition for vertexing with Layer 0.

Long range tails of the HPS beam generate measurable occupancies in Layer 1 which will be larger in Layer 0 due to the proximity of the beam. Measurements of the beam tails using Layer 1 of the SVT in the engineering run fitted to a Gaussian, as shown in Figure 6, predict that the resulting occupancy at the edge of Layer 0 will be roughly similar to that in Layer 1 after accounting for the reduction from splitting the readout strips. While this occupancy

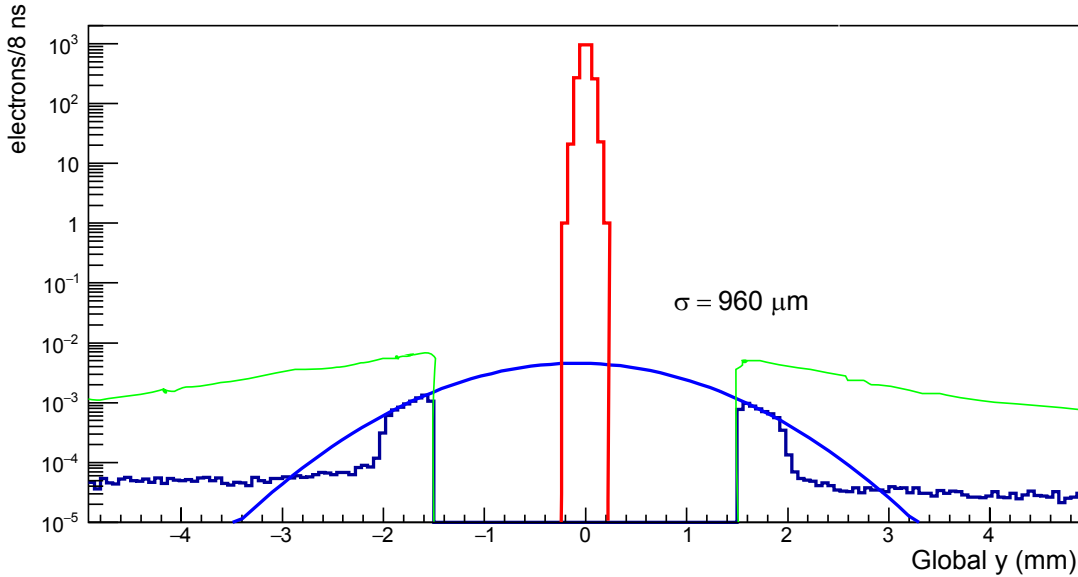


FIG. 6: The particle occupancy per 8 ns during normal operation with the target (green) and without the target present (blue) as measured in Layer 1 both above and below the beamline. Also shown is the flux corresponding to a narrow 50 nA beam centered at $y=0$ (red). A collimator blocks the beam tails beyond ± 2 mm, but the profile of occupancy above and below the beam are used to extract the gaussian profile of the beam halo (fit), which has a width of approximately 1 mm. This measurement implies backgrounds from beam halo at 0.75 mm from the beam about double that at 1.5 mm.

will be acceptable at lower currents, it could become a limiting factor for operation of the SVT at the high currents envisioned for running at 4.4 GeV and 6.6 GeV in both Layer 0 and Layer 1. Therefore, further study will be required to assess the impact of beam tails on the vertexing reach at higher running energies and what mitigations may be possible. In the worst case, lower currents and longer running times might be required to enable HPS to deliver the best vertexing reach at higher beam energies.

In order to achieve the desired material reduction, the silicon must be half as thick as

that in the other layers of the SVT, or roughly $150\ \mu\text{m}$ of silicon with no support. While such silicon is available from a number of vendors, the more significant issue is that thinning the silicon results in a commensurate loss of signal. The ability to fit periodic samples of the shaped signal pulses to extract the hit time with a precision of $\approx 2\ \text{ns}$ is fundamental to reducing un-triggered, random backgrounds in the SVT to acceptable levels for high-purity vertexing. Since hit time resolution degrades rapidly for $S/N < 20$, the loss of signal from thin silicon must be compensated with lower noise. [13] This is naturally achieved with smaller sensors, since studies show that the Layer 0 sensors can be as short as 2 cm and achieve full efficiency for both A' decay daughters and recoiling electrons, as shown in Figure 7. With

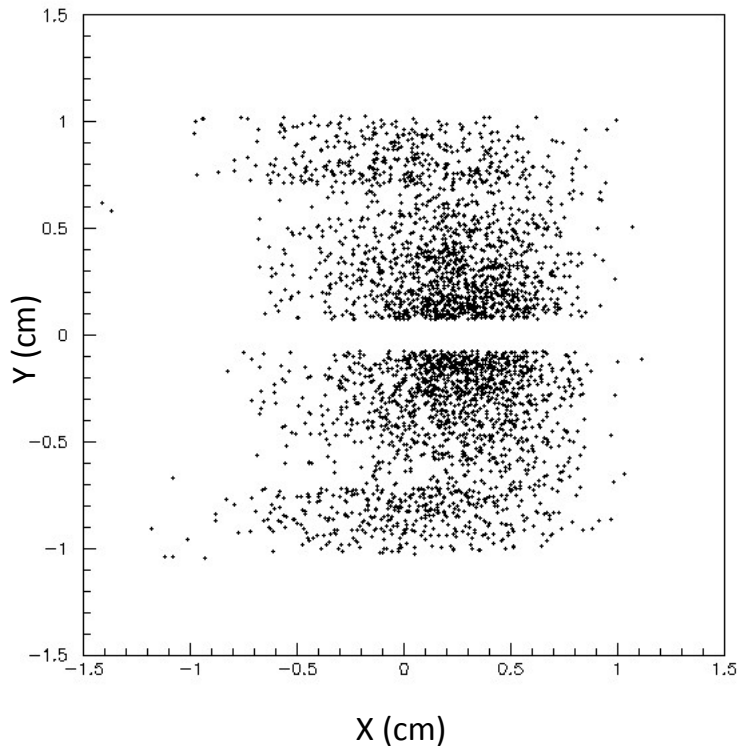


FIG. 7: The distribution of hits from electron recoils that also produce hits in Layers 1 and 2. Together with the beamspot constraint, such recoils can be reconstructed with high efficiency. Including the recoil in a kinematic fit significantly increases the sensitivity of the resonance search.

readout strips split in half to reduce occupancy, as previously described, the noise will be approximately $1/3$ that of the other layers of the SVT for the same readout technology, resulting in even higher S/N than in the rest of the SVT. It is important to remember that lowering both signal and noise in Layer 0 will result in lower readout thresholds. Because of this, the 10 keV L-shell x-rays generated from the action of the beam on the tungsten target

will deposit enough energy in the silicon to consistently pass threshold cuts, in contrast to the situation in Layer 1 where these x-rays are at or slightly below threshold in most channels. Simulations show that the small size of the sensors for Layer 0 together with thickness that results in only $\approx 70\%$ absorption at this energy in each sensor give rise to less than 1/2 hit in Layer 0 per 8 ns time window. This uniform 0.07% occupancy has no significant effect on tracking performance.

The background from scattered beam electrons dominates the radiation dose to the sensors that limit their lifetime through bulk damage effects proportional to the areal density of hits. Sensors in the same technology used in the rest of the SVT will last only 25% as long as in Layer 1, or approximately six weeks for silicon of the same thickness and operating at the same voltage. Given the short run periods expected for HPS, such a short lifetime may be acceptable with planned periodic replacement of Layer 0. However, 150 μm silicon, operable at the same voltage as the rest of the SVT, will withstand double the radiation dose, extending the lifetime of sensors in Layer 0 to three months.

For the project to be feasible, it must fit within the existing mechanical and DAQ framework of the SVT. This requirement is easily accommodated, since the upper and lower cooling structures of the SVT extend upstream to approximately $z = 5$ cm, where Layer 0 would be mounted and where the SVT beam scan wires are currently located, as shown in Figure 8. By moving the scan wires slightly upstream the same wire supports can be reused in the upgraded detector. Meanwhile, the DAQ for the current SVT has the excess capacity needed to accommodate the new layer. Inside the vacuum chamber, this includes connectivity for the modules on the cooling structures between Layers 1 and 2, the Front End Boards (FEBs) that provide control and power to the modules and digitize signals from them, and the optoelectronic vacuum feedthrough boards that relay signals from the FEBs to the remotely located RCE DAQ and power supplies. In short, the entirety of the power and DAQ needed for Layer 0 was already installed and tested in the SVT and SVT DAQ as originally built.

2.1 Mechanics

There are two significant mechanical projects to be undertaken in the Layer 0 upgrade. The first is the design and assembly of the new sensor modules, including the sensors,

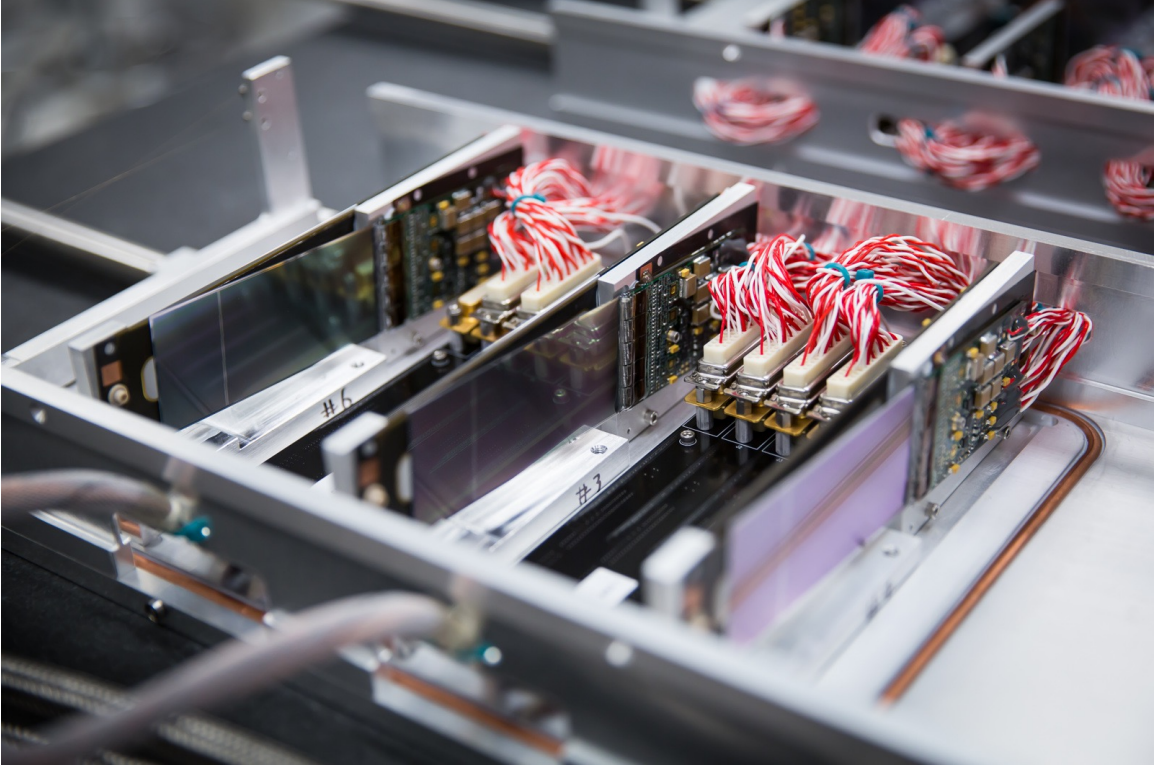


FIG. 8: A photograph of the u-channel support structure that holds the Layer 1-3 modules of the SVT. Layer 0 would be mounted on this support in roughly to same position as the wire scanner support seen at left, with scan wires moved slightly upstream towards the target. The crossover boards that provide power and readout for the modules can be seen between the SVT modules, where the two unused connections on the crossover board between Layers 1 and 2 can be used for Layer 0.

the APV25 hybrids and the aluminum module supports. The second is the integration of these modules into the existing mechanics of the SVT, namely the u-channels that hold the modules of Layers 1-3 and the SVT scan wires.

A conceptual design for a module is shown in Figure 9. Because the sensors are so small and have readout from both ends, it is both possible and very desirable to have both ends of the sensor read out by the same hybrid circuit board so that both ends of the sensor have a low impedance connection to the same references for ground and bias. To achieve this, the rectangular hybrid will have a cutout along one edge and the sensor will be glued directly to the periphery of this cutout, as shown in Figure 10. It is not anticipated that thermal expansion and contraction will be significant issues given the small size of the sensors, but testing will be performed to ensure that this is the case and a flexible silicone elastomer adhesive may be used if there are issues. There is no carbon fiber backing in the design, for

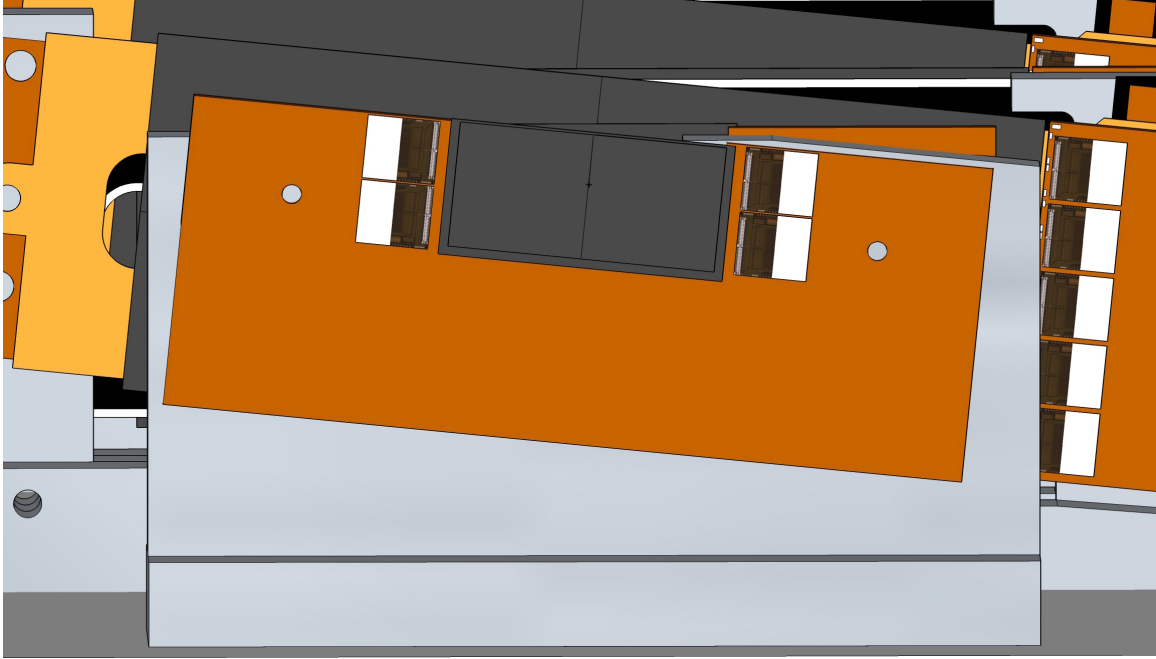


FIG. 9: The conceptual design for the Layer 0 modules and module supports.

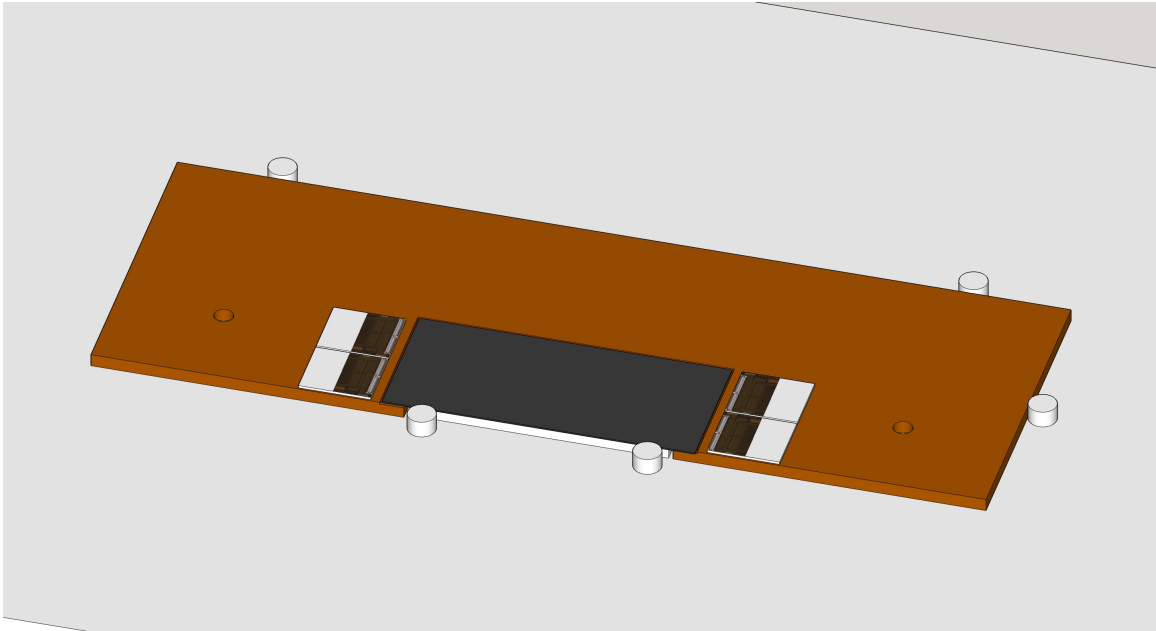


FIG. 10: The conceptual design of the Layer 0 hybrids. The sensor is mounted on the step in the window of the hybrid.

simplicity and to minimize material, but the heat path to the hybrid is very short, and there is cooling around the entire periphery of the sensor unlike the rest of the detector where cooling is only provided from the ends of the modules.

The bias voltage to the back of the sensor will be supplied by a pad on the surface of the

hybrid along the long edge of the sensor, with connection via silver epoxy joint. Around the rest of the periphery, there will be passivated thermal vias that carry heat from the sensor to the backplane of the hybrid, where thermal compound will be used to ensure good thermal conductance to the aluminum module support. The hybrid will be positioned by pins along one edge and at one end during attachment of the sensor, which will also be positioned by a pair of pins determining the sensor position and rotation in the measurement coordinate relative to the hybrid. In the other coordinate, along the strip direction, the sensors will be positioned by a step in the hybrid, which should be sufficient to determine the position in the non-measured coordinate to about 100 microns. The module supports will have pins to position the hybrids in the exact same location as the positioning pins used during sensor attachment. Even though the hybrids are not precision components, referencing the exact same locations at the hybrid edges should ensure relative positioning at the 25 micron level for position in the measurement coordinate along the length of the sensor, which is critical to ensuring the clearance between the edge of the Layer 0 silicon and the CEBAF beam.

The new modules will need to be mounted on the “lever blocks” which are mounted to the baseplates of the Layer 1-3 U-channels. The current lever block includes a clamp for the SVT motion levers as well as precision mounting points for the frames that hold the SVT scan wires. It does not appear that there is room for both the Layer 0 modules and the wireframes on the current lever blocks, so slightly longer lever blocks will need to be produced that extend 1-2 cm further upstream to accommodate both Layer 0 at $z=5$ cm and the scan wires between Layer 0 and the target at $z=0$ cm. In principle, the new lever blocks can simply be a slightly stretched version of the existing design with new mounting points for the Layer 0 module similar to those included in the baseplates of the u-channels for the rest of the layers. Although no special provisions were made for ensuring good cooling of the lever block in the existing SVT, the supply path of the copper cooling line is pressed into the u-channel directly underneath the lever block where Layer 0 will sit and runs lengthwise under the module support. Therefore, addition of thermal compound during assembly should ensure more than adequate cooling for Layer 0, which totals less than 3 W each for the top and bottom u-channels.

Finally, the shims for moving the modules of Layers 2 and 3 closer to $y=0$ will be fabricated from non-magnetic shim stock, where only clearance holes are needed to accommodate the hardware used to position and attach the modules to the U-channels. The shims are

sufficiently thin that no changes to the hardware used to mount the modules are anticipated. The scope of this work is so small that changes to the plan to move Layers 2 and 3 may be considered until near the end of the upgrade project.

2.2 Sensors

The silicon sensors for Layer 0 are similar to those used in the rest of the SVT, being fabricated on p⁺-in-n bulk, $\langle 100 \rangle$ silicon designed to withstand high bias voltages. Unlike the sensors used in the rest of the SVT, the sensors for Layer 0 will be thinned (150 μm vs. 320 μm), have a slim edge (≤ 200 μm vs. 1 mm), and will have strips that are divided in the center of the sensor, splitting the sensor in two with readout at both ends. Because the sensors are designed to be used very close to the target, they may be much smaller than the rest of the sensors in the detector. The dimensions and properties of the sensors are shown in Table I.

The sensors will be designed and fabricated by the CNM campus of D+T Electronics with whom we have considerable experience in fabricating similar devices, according to written specification with which they have been provided for a quotation.

2.3 Data Acquisition

The only component being produced for the data acquisition are the new Layer 0 hybrids. As mentioned in the introduction, there are unused DAQ channels with connectors on the Layer 1-3 U-channels that are fully supported by hardware throughout the DAQ chain. However, the unused channels will need to be tested to ensure that they are functioning properly and new firmware, control software and event model software will need to be developed to support taking data with all channels of the DAQ. The hybrids themselves will be of similar construction to those for the other Layers. With only four APV25 chips, the hybrids will be somewhat simpler and require fewer components, but because the sensors are so small, the surface area on the hybrid is not very constrained relative to the other layers. In order to allow Layer 0 to be plugged into the existing crossover boards, the new hybrids will need to utilize soldered pigtails terminated in DB25 connectors similar to those used in the Layer 1-3 modules originally constructed for the HPS Test Run and routing of these

Attribute	Specification
Wafer size	4-in. (100 mm)
Wafer type	n-type FZ
Wafer orientation	$\langle 100 \rangle$
Wafer thickness (after thinning)	$150 \pm 10 \mu\text{m}$
Wafer thickness tolerance	5%
Wafer active thickness	$\geq 90\%$ of physical thickness
Wafer resistivity	$> 1.5 \text{ k}\Omega\text{cm}$
Full depletion voltage	$< 50 \text{ V}$
Maximum operation voltage	500 V
Inner dimension	$14 \times 30 \text{ mm}^2$
Sensor bow after process and dicing:	$< 200 \mu\text{m}$
Strip segments	2
Number of strips in a segment	255
Strip segment length (approximate)	14.9 mm
Strip implant	P
Strip pitch	$55 \mu\text{m}$
Gap between strip segments	$\leq 55 \mu\text{m}$
Strip readout coupling	AC
Strip readout metal	Pure Aluminum
Strip AC coupling capacitance	$> 20 \text{ pF/cm}$
Resistance of readout Al strips	$< 100 \Omega/\text{cm}$
Resistance of N-implant strips	$< 200 \text{ k}\Omega/\text{cm}$
Strip bias resistor	Polysilicon
Strip bias resistance (R_b)	$1.0 \pm 0.5 \text{ M}\Omega$
Interstrip resistance (R_{int})	$> 10 \times R_b$ at 300 V at RT
Number of strip defects	$< 1\%$ per strip/segment, $< 1\%$ per sensor
Leakage current	$< 1 \mu\text{A}/\text{cm}^2$ at 200 V at RT

TABLE I: A summary of the specifications for the Layer 0 sensors.

pigtails around Layer 1 to connect to the crossover boards will be difficult. In the worst case, additional routing slots for the pigtailed will need to be machined in the side plates for the U-channels to accommodate the mass of cables, but this is a small job with minor consequences.

2.4 Installation and Integration

In order to perform the required work on the U-channels they will need to be disassembled. While it might be possible to safely perform the required work with Layer 1-3 in place, even removal of the lever block may endanger the safety of the modules. Furthermore, the modules of Layers 2 and 3 will need to be removed in order to add shims underneath to increase the

acceptance of the SVT for long-lived decays. Meanwhile, Layer 0 will need to be surveyed to determine its position relative to the SVT scan wires and Layers 1-3, just as the U-channels were originally surveyed after assembly and before installation of the SVT. While it may, in principle, be possible to undertake this work at JLab, it makes far more sense to perform the work at SLAC, along with the DAQ development and testing, if at all possible.

For this reason, we expect to bring the Layer 1-3 U-channels back from JLab for this work. Fortunately, this is relatively simple, because the Layer 1-3 U-channels can be disconnected and extracted from the vacuum chamber without removing the entire SVT package, and there is a custom shipping crate for the Layer 1-3 U-channels at JLab which can be used to safely ship them back and forth between JLab and SLAC. Because the largest components to be tested are these U-channels, we anticipate that all work at SLAC can be done in the Building 84 cleanroom.

3 HPS SVT Upgrade Project Outline and Scope of Work

The outline of the project is defined by the following sub-projects.

1. transportation of Layer 1-3 U-channels from JLab to SLAC
2. disassembly of U-channels and storage of modules and scan wireframes
3. design, procurement, processing and testing of Layer 0 sensors
4. design, procurement, assembly and testing of Layer 0 hybrids
5. assembly and testing of Layer 0 modules
6. design, procurement, assembly and testing of Layer 0 module supports
7. design, procurement, and testing of new U-channel lever blocks
8. assembly and survey of U-channels with lever blocks
9. design, procurement, and testing of shims for Layers 2 and 3

10. mounting L0-L3 modules and scan wireframes on U-channels
11. final testing of U-channels
12. survey of U-channels
13. transportation of upgraded U-channels from SLAC to JLab
14. installation of upgraded U-channels in SVT
15. final testing and survey of upgraded SVT

3.1 Schedule

A schedule for the Layer 0 upgrade is shown in Figure 11. This schedule assumes project start on 6/15/17, which begins with procurement of the silicon sensors. The entire engineering task for the project, along with procurement, assembly and testing of the hybrids and support structures are in the shadow of the silicon procurement with approximately 25% contingency, so the silicon procurement drives the critical path until the silicon has arrived and module assembly begins. The time assumed for module assembly is conservative given that the upgraded detector can be completed once four good half-modules are in hand. Because we may need to replace these modules after they are damaged by radiation from operation in the beam (lifetime may be as short as three months), we plan to produce a large number of spares (at least 8 half-modules) with the rest of the time shown in the schedule. All estimates are based on previous experience with design and fabrication of similar components, assembly and testing work using the same processes, and procurement times with the required vendors.

3.2 Budget

The required budget for the SVT upgrade is shown in Figure 12. The budget is dominated by labor, and in particular professional labor required for engineering the electronics and mechanical elements of the upgrade. Professional labor is budgeted as quoted by TID AIR for electronics work and based on previous experience for mechanical work. Most of the

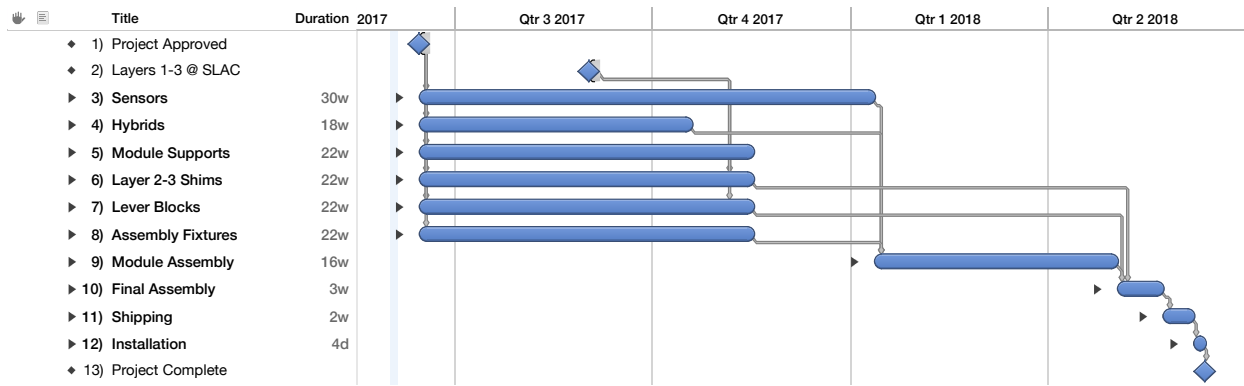


FIG. 11: The schedule for assembly of the SVT upgrade, with only high-level tasks shown.

assembly and testing labor will be performed by scientists and students. M&S items are costed based upon quotes and previous work on the SVT, where significant contingency is included on items for which there is no direct quote on record. A single item, the hybrid circuit board procurement, carries 100% contingency based upon previous experience so that a second hybrid order is possible. The sensor, a significantly new item, is costed using a direct quote from the vendor, with whom UCSC has significant previous experience and a close working relationship.

	Labor	M&S	Totals
Sensors	\$5000	\$37500	\$42500
Hybrids	\$64360	\$10000.00	\$74360.00
Modules	\$75640	\$10000.00	\$85640.00
U-channels	\$61640	\$10000.00	\$71640.00
Misc	\$5000	\$5000.00	\$10000.00
TOTALS	\$211640	\$72500.00	\$284140.00

FIG. 12: The proposed budget for the SVT. All work and components, with the exception of the sensors, are very similar to those previously used in the SVT, and include at least 25% contingency. The sensor costs are based upon a direct quote from the vendor.

The project anticipates getting started very quickly, beginning with the sensor order and all major engineering items, both electronic and mechanical, completing in 2017, along with assembly of the hybrid circuit boards. In this scenario, the funds required in FY17 are \$124K, assuming sensor payment due on delivery falling in FY18. The remaining project cost of \$150K would fall in FY18. However, if approvals delay the project start significantly,

the engineering and hybrid assembly tasks will begin to push into FY18 by an amount roughly proportional to the number of days remaining in FY17 after project start. Included funds required for work at UCSC are roughly 50% in each fiscal year (\$14K each), with the same caveat.

-
- [1] B. Holdom, Two $U(1)$'s and Epsilon Charge Shifts, *Phys.Lett.* **B166**, 196 (1986).
 - [2] P. Galison and A. Manohar, TWO Z 's OR NOT TWO Z 's?, *Phys.Lett.* **B136**, 279 (1984).
 - [3] R. Essig, J. A. Jaros, W. Wester, P. H. Adrian, S. Andreas, et al., Dark Sectors and New, Light, Weakly-Coupled Particles, 2013.
 - [4] M. Pospelov, Secluded $U(1)$ below the weak scale, *Phys.Rev.* **D80**, 095002 (2009).
 - [5] O. Adriani et al., An anomalous positron abundance in cosmic rays with energies 1.5-100 GeV, *Nature* **458**, 607–609 (2009).
 - [6] M. Ackermann et al., Measurement of separate cosmic-ray electron and positron spectra with the Fermi Large Area Telescope, *Phys.Rev.Lett.* **108**, 011103 (2012).
 - [7] M. Aguilar et al., First Result from the Alpha Magnetic Spectrometer on the International Space Station: Precision Measurement of the Positron Fraction in Primary Cosmic Rays of 0.5350 GeV, *Phys.Rev.Lett.* **110**, 141102 (2013).
 - [8] N. Arkani-Hamed, D. P. Finkbeiner, T. R. Slatyer, and N. Weiner, A Theory of Dark Matter, *Phys.Rev.* **D79**, 015014 (2009).
 - [9] M. Pospelov and A. Ritz, Astrophysical Signatures of Secluded Dark Matter, *Phys.Lett.* **B671**, 391–397 (2009).
 - [10] J. D. Bjorken, R. Essig, P. Schuster, and N. Toro, New Fixed-Target Experiments to Search for Dark Gauge Forces, *Phys.Rev.* **D80**, 075018 (2009).
 - [11] P. Hansson Adrian et al., Heavy Photon Search Experiment at Jefferson Laboratory: proposal for 2014-2015 run, 2013.
 - [12] V. Fadeyev et al., Update on scribe–cleave–passivate (SCP) slim edge technology for silicon sensors: Automated processing and radiation resistance, *Nucl. Instrum. Meth.* **A765**, 59 – 63 (2014).
 - [13] M. Friedl, C. Imler, and M. Pernicka, Obtaining exact time information of hits in silicon strip sensors read out by the APV25 front-end chip, *Nucl. Instrum. Meth.* **A572**(1), 385 –

387 (2007).